Elsevier Editorial System(tm) for
International Journal of Mineral Processing
Manuscript Draft

Manuscript Number: MP-14-317R2

Title: Discrete X-ray tomographic reconstruction for fast mineral liberation spectrum retrieval.

Article Type: Research Paper

Keywords: mineral liberation
X-ray tomography
particulate characterization
discrete algebraical techniques

Corresponding Author: Dr. G. Schena,

Corresponding Author's Institution: University of Trieste

First Author: G. Schena

Order of Authors: G. Schena; Marzio Piller; massimiliano Zanin

Abstract: In minerals beneficiation, the mineral liberation spectrum of the plant feed is valuable information for adjusting operations, provided the information is available in minutes from particulate sampling. X-ray micro-tomography is the only technique available for unbiased measurement of composite particles composition (on a 3D basis). The bottleneck of current micro-tomographic systems is the X-ray scanning time (data acquisition) rather than the slice reconstruction time (data processing). An algorithm capable of reconstructing tomographic slices of composite mineral particles from a limited number of radiographic projections, and therefore significantly reduce the overall measurement time, is presented and demonstrated with numerical examples. The algorithm is cast around the discrete algebraical reconstruction technique and requires less than one tenth of the projection data required by the currently used filtered back-projection methods, thus allowing a dramatic reduction of the scanning time.

Cover Letter

YOUR REF. No.: MP-14-317R1

Paper title: Discrete X-ray tomographic reconstruction for fast mineral liberation spectrum retrieval.

Second revision of the paper submitted to International Journal of Mineral Processing,

Prof. Maurizio L. Torem

Editor in Chief

International Journal of Mineral Processing

Dear Prof. Maurizio Torem,

Please find herewith the second revision of the paper MP-14-317 (R1).

The remarks of the reviewer were pertinent and we have modified the paper accordingly.

We added sub-section 2.1.1. that precisely addresses the request of the Reviewer of explain how to extend the use of the proposed methodology to the case with more than two mineralogical species.

The rest of the paper remains unchanged with the exception of minor alterations related to a thorough spelling.

I have loaded the MS Word file with the figures incorporated for an easy re-reading and separately a copy of the original high quality figures.

Regards,

Gianni Schena

Corresponding author.

Trieste, 22 September 2015

YOUR REF. No.: MP-14-317**R1**

Paper title: Discrete X-ray tomographic reconstruction for fast mineral liberation spectrum retrieval.

Second revision of the paper submitted to International Journal of Mineral Processing,

Dear Reviewer2,

Please find herewith the second revision of the paper MP-14-317 (R1).

The remarks you made were pertinent and we have modified the paper accordingly.

We added sub-section 2.1.1. that precisely addresses your request of explaining how to extend the use of the proposed methodology to the case with more than two mineralogical species.

The rest of the paper remains unchanged with the exception of minor alterations related to a needed thorough spelling.

Thank you very much for your time.

Regards,

Gianni Schena

Corresponding author.

Trieste, 22 September 2015

Highlights

. X-ray tomography is a promising tools for un-biased mineral liberation studies

. A reconstruction method that uses few projections for generating a slice is proposed

. An original approach is used and the reconstruction solved by binary programming

. The scanning-time is cut and mineral liberation data generated in shorter time

. Results of numerical experiments are compared to traditional reconstruction methods

*Manuscript
Click here to download Manuscript: ijmp_liberation_DART_2nd_rev_MP-14-317_R1_.doc Click here to view linked References

Title:
Discrete X-ray tomographic reconstruction for fast mineral liberation spectrum retrieval.

Authors: Gianni Schena*, Marzio Piller , Massimiliano Zanin

Email: {schena,piller}@units.it [(1)] , massimliano.zanin@unisa.edu.au[(2)]

Affiliation:

[(1)]Dept. of Engineering and Architecture,

University of Trieste, 34127, Trieste, Italy

[(2)]Ian Wark Research Institute,

University of South Australia, Mawson Lakes SA 5095, Australia

*Corresponding author.

E-mail address: schena@units.it (Gianni Schena)

Date: Received July 7 2014, in revised form June 2015

Abstract

In minerals beneficiation, the mineral liberation spectrum of the plant feed conveys valuable information for adjusting operations, provided it is available in minutes from particulate sampling. X-ray micro-tomography is the only technique available for unbiased measurement of composite particle composition (on a 3D basis). The bottleneck of current micro-tomographic systems is the X-ray scanning time (data acquisition) rather than the slice reconstruction time (data processing). An algorithm capable of reconstructing tomographic slices of composite mineral particles from a limited number of radiographic projections, thus significantly reducing the overall measurement time, is presented and demonstrated with numerical examples. The algorithm is cast around the *discrete algebraical reconstruction technique* and requires less than one tenth of the projection data needed by the currently used filtered back-projection methods, thus allowing a dramatic reduction of the scanning time.

Keywords:

mineral liberation, X-ray tomography, tomographic reconstruction, discrete algebraical techniques

1.Introduction

The metallurgical performance (metal recovery and concentrate grade) of an operating plant is determined by the liberation spectrum of the particles undergoing concentration and by the efficiency of the separation process. Ideally, maximum separation efficiency is achieved when particles are fully liberated. In practice, optimum liberation is always a compromise between ore mineralogy and energy required for comminution. The latter is often the most energy intensive and costly operation thus capable of compromising the profitability of the entire beneficiation process. In this contest, the possibility to assess the minerals

liberation in the feed to the plant is a key factor for tuning the grinding systems at one side and to adjust the separation circuit at the other side. The potential of process mineralogy and automated laboratory characterization is recognized both by academia and industry (Baum, 2014). In short, fast automated mineralogy is a necessary component of modern control strategies able to respond to fluctuations in grade, mineralogy and texture that can be detrimental to metallurgical performance.

The combined use of SEM measurements of areal-grades (QEM-Scan) or linear intercepts on transects (MLA) of polished sections of the particles is popular to assess mineral liberation. However, these methods provide biased estimates of liberation (G. Barbery, 1991). The stereological correction methods for converting (e.g. via kernel correction) these low dimensional measurements into volumetric grade distributions are complex and not well established procedures (G.M. Leigh, 1993 ; C. Chiaruttini et al., 1999). In addition, these kernel correction procedures require time consuming sample preparation and measurements and are not free of error.

The use of X-ray micro-tomographic systems specifically designed for this purpose is very attractive. The principle of X-ray computed tomography is conceptually simple: the X-rays are attenuated differently while traversing the composite particles. The intensity of the X-ray signal is converted by a scintillator into light and recorded by a camera as a radiographic digital image. The object is then rotated by small angular steps and the radiographic operation repeated each time until completing full rotation. The collection of several hundred projections is employed to reconstruct the inner structure of the particles.

Commercial tomographic system are available from a number of makers but a tomographic system can easily be built in-house by assembling the three basic components (one cone beam micro-focus X-ray source, one traditional CCD or CMOS based X-ray digital camera or flat panel, and one precision air-bearing rotation stage) in a lead-wall cabinet for X-ray shielding.

Prof. J. Miller's research group at University of Utah introduced the micro CT system into the mineral processing laboratory (C. Lin et al.,1996 ; J.D. Miller et al., 2003). Today this technique is recognized as capable of supporting the engineers in the study of a number particulate processes encountered in mineral- and hydrometallurgy-operation. It has been used in typical mineral processing analysis such as washability and mineral liberation, to observe particulate leaching advancement (N. Dhawan et al., 2012), to evaluate separation efficiency, to observe filter-caking formation (C. Lin et al.,2000), to reconstruct the full morphology of porous rocks to simulate fluid multiphase flow through pores and throats (D. Casagrande et al., 2014, M. Piller et al., 2014). In short, micro CT is helpful where information on the inaccessible internal composition of particles is necessary to supplement the biased observation conveyed by measurements on particle surfaces or on low-dimension particle sectioning (i.e. linear intercepts or areal grades). Low dimension measurements invariably overestimate the liberation: they could see only one phase in a two-

phase particle. This new quantitative tomographic technique is now available in a few leading mineral laboratories but once disseminated and with well-established operating protocols it will be capable to provide data superior to those traditionally provided by mineralogical observations on particle-sections or to supplement their information content. The micrometric spatial resolution of X-CT and the capability of detecting low density-contrast permits 3D textural characterization. The authors of this paper have also explored the use of CT both at synchrotron beam-lines and with laboratory micro-focus sources (G. Schena et al., 2003, 2007). Its potential for sorting and micro-diamond detection was also explored (G. Schena et al., 2005).

Unfortunately, the current tomographic systems are not yet fast enough to provide liberation data in a few minutes or less, as desirable for a practical use in plant operations. The bottleneck is the scanning time required to take a sufficient number of radiographic projections with a full coverage around 360 degrees of the rotating sample. Often, several hundred projections need to be taken to satisfy the minimum sampling requirements of the filtered back projection (FBP) algorithm that is the standard slice reconstruction method. The minimum number of projections prescribed to strictly respect the Nyquist sampling frequency principle is: number of projections$= \frac{\pi}{2}\mathrm{D}$, where D is the diameter of the object in pixels. Today, the tomographic slice-reconstruction time is not a hurdle as in the past; many commercial codes are implemented on graphic board hardware for fast processing the radiographic projections to reconstruct the slices. It is the high number of projections required for reconstruction which still is an issue.

Roughly, one can envisage that even with a routinely and well-established workflow protocol for sampling, scanning, reconstructing and post-processing the tomographic digital volume, not less than a few hours are necessary for having the liberation data available for decision making. Most of the time burden is ascribed to X-ray scanning. When the number of projections is less than the prescribed minimum, the filtered back projection yields a reconstruction that is pathologically affected by radial streak artifacts and unsuitable for automatic image analysis procedures.

The alternative strategy proposed herewith is to reconstruct the tomographic slices with a method that is much less demanding in terms of number of radiographic projections and thus appropriate to cut the scanning time and in turn the overall time required for having usable liberation data. The method uses prior-knowledge of the attenuation of the mineral species that can be easily acquired with one single standard tomography. The novelty proposed is in the slice-reconstruction algorithm. Therefore, the method does not require any modification of the hardware of the existing tomographic scanning machines. Indeed, prior knowledge of the single mineralogical species allows introducing the additional constraints needed to significantly reduce the number of projections required for a high quality segmented reconstruction.

2.Discrete algebraical reconstruction technique

Rather than de-convolving the integral information content of the projections with the inverse of the Radon transform and its filtered back-projection implementation (Xiaochuan Pan et al., 2009), we set-up the slice image reconstruction problem according to the so called algebraical reconstruction technique (ART). We aim to reconstruct the image by minimizing the difference between the given projection data acquired from scanning and the (forward) projections of the image under reconstruction. The data fidelity (equality) constraint is written as a linear set of equations where the right side is the projection data (see Eq. (1) in the next section). The sketch in Fig. 1 illustrates the correspondence between pixels and coefficients of the linear equations according the ART framework. For illustration purposes only horizontal (Θ=0°), diagonal (Θ=45°) and vertical (Θ=90°) rays are shown. The pixels of the 4x4 sought image are row-wise numbered from 1 to 16. The continuous ART is also known as Projections onto Convex Set (POCS); the convex set is defined by the constraining hyper-planes. One commercial implementation of ART for continuous tomography exists (www.digisens3D.com).

When the solution sought should take discrete values the method is referred to as Discrete Algebraical Reconstruction Technique (DART). A vast literature exists on the DART methods where a binary (0,1) solution is required (G.Herman and A.Kuba, 2007), e.g. for applications where it is required to discriminate between one material and voids. Much less literature exists for applications similar to that proposed in this paper where liberated particles and composite particles made up of more mineral species are to be segmented based on their different X-ray attenuation as recorded by the projections (van Aarle et al., 2012, Batenburg and Sijbers, 2011) by discrete tomography techniques.

The constraint prescribing that the sought image should contain pixels taking luminosity in a small discrete set is an extremely valuable *a priori* information and allows to reconstruct using few tomographic projections.

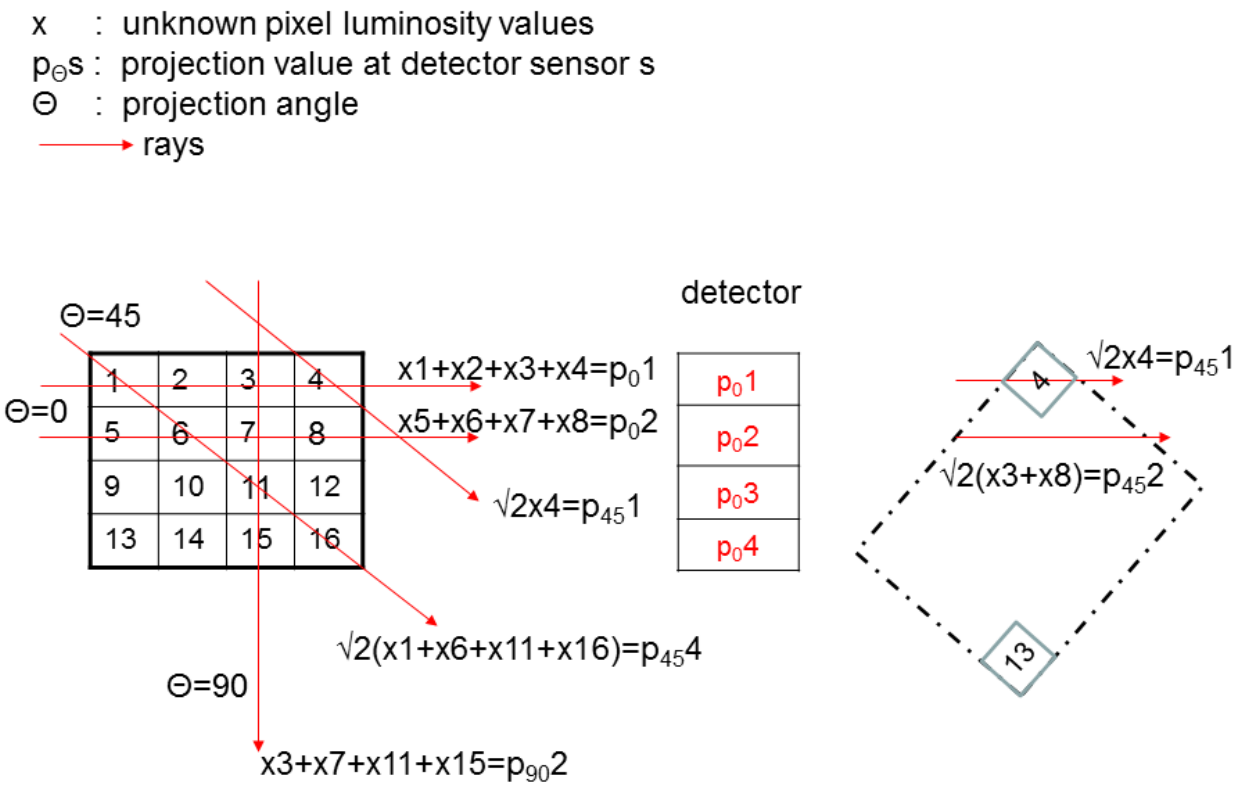

Fig. 1. Algebraical reconstruction technique framework for a 4x4 tomographic slice.

2.1.Numerical method.

The number of columns of the ART system matrix is the number of pixels of the square (NxN) image to reconstruct (see Fig. 1). The number of equations is the number of rays times the number of projection angles.

Formally, for continuous tomography, the ART equality constraints are:

$$Sx = p \quad or \quad \sum_{j=1}^{N^2} s_{i,j} \; x_j \; = \; p_i \tag{1}$$

where:

x is the column vector of pixel values of the sought image, the ((n-1)N+m)-th entry of x is the (n,m)-th pixel location of the NxN slice image,

S is the sparse, real-valued matrix of the severely under-determined tomographic reconstruction problem,

p is the projection vector.

In short, the ij-th element of the system matrix S is non-zero if the i-th ray beam passes through the j-th pixel. Normally the sample undergoing tomography is a cylinder then only the coefficients corresponding to a disk contained in the square image domain of the slice are non-zero. S is sometime referred to as tomographic projection matrix. The element $s_{i,j}$ is the contribution of the pixel j to the measurement i, and it is the intersection length between the pixel j and the projection ray i, $\sqrt{2} \geq s_{i,j} \geq 0$.

In practice, in an operating plant the mineral species and their attenuation are known and the sought slice image has a discrete number of gray levels. Thus the pixel values in the vector x (see Eq.(1)) are bound to take discrete values. The discrete nature of the image constitutes an element of simplicity that is capable of further constraining the solution of Eq. (1). Thus transforming the continuous ART into a Discrete ART (i.e., DART) reconstruction problem.

To simplify the formalization we assume, at this stage, that composite particles are made up of two mineral phases: a high density valuable phase with attenuation H and a low density phase with attenuation L. The feasible values of the unknown vector are {0 , L , H}. The value 0 represent the void. However, the model can be extended to more than two solid phases as untangled in section 2.1.1.

The general terms of the i-th equality constraint of the original continuous ART problem is:

$$\dots s_{i,j}\, x_j \dots = p_i \tag{2}$$

By introducing a change of variable the equality can re-written as a Discrete ART (DART) problem.

$$\dots s_{i,j}\, L\, y_k + s_{i,j}\, H\, y_{k+1} \dots = p_i \tag{3}$$

where for j=1 then k=1 , for j>1 then k=j·2-1 and j is in the range 1 to N^2. The new variable y is boolean.

In addition, the system of equations (3) in the new variable *y* should be augmented *appending* the inequalities:

$$y_k + y_{k+1} \leq 1 \tag{4}$$

that should be imposed for each k. These constraints (4) prescribing that a pixel can be H or L or 0 (see Eq. (5)).

The DART problem is solved as a Boolean problem, with y taking values in {0 , 1}. The binary solution y is then post processed as:

$$\begin{cases} \text{if } y_k = 0 \; and \;\; y_{k+1} = 0 \; then \; x_j = 0 \\ \text{If } y_k = 1 \; and \;\; y_{k+1} = 0 \; then \; x_j = L \\ \text{If } y_k = 0 \; and \;\; y_{k+1} = 1 \; then \; x_j = H \end{cases} \tag{5}$$

And x -the vector of the pixel values of the reconstructed slice image- is retrieved. The image that arises from the solution of Eq.s (3 -4) in y ,further post-processed with (5) is already segmented into three gray values: 0, L, H.

In contrast, images reconstructed with continuous tomography have real valued pixels and require further filtering and the use of threshold and segmentation procedures to allocate the pixels to the void or to one of the two mineralogical phases with different x-ray linear attenuation coefficients.

Eq.(3) can be equivalently and conveniently re-written as system of linear inequality constraints:

$$-\epsilon_i \leq \ldots s_{i,j} \, L \, y_k + s_{i,j} \, H \, y_{k+1} \ldots - p_i \leq \epsilon_i \qquad , \qquad i = 1, \ldots, N \tag{6}$$

where **ϵ** ($\boldsymbol{\epsilon} \geq 0$) is a suitable small parameter allowing violation of the equalities in Eq.(3). This new formulation transforms (3) into a constrained linear programming problem that can be solved resorting to specialized software.

For the solution of Eq. (6) supplemented with Eq. (4), we used IBM ILOG Cplex that is a suite of state of the art solvers for linear programming problems and includes the binary solver *cplexbilp*. Independent benchmarks show that CPLEX outperforms most of the commercial and open source competitors (see benchmark tables produced and continuously updated by Prof. Hans D. Mittelmann at http://plato.la.asu.edu/).

As a tutorial and illustrative example, the sparsity pattern of the matrix of constraints (see Eq. (3)) is reported in Fig. 2. The example assumes one 4-pixel side image to reconstruct. Only horizontal, vertical and diagonal projections are considered. The original S matrix in Eq.(2) is 16 columns and after the change of variables (see Eq.(3)) the new constraint matrix is formed by 32 columns. The *appended* banded lower section Eq.(4) of the full matrix is omitted for visualization purposes. In Fig. 2, also the value of the coefficients of the 32 columns matrix is visualized with the diameters of the red circles at the position where $s_{i,j}$ >0. In the illustrative example L=1, H=2: $s_{i,j}$ is 0 or 1 for the horizontal and vertical projection and $\sqrt{2} \geq s_{i,j} \geq 0$ for the diagonal projection (see Fig. 1).

The fraction of non-zero elements over the total number of elements in real S matrices is often of 10^{-3}.

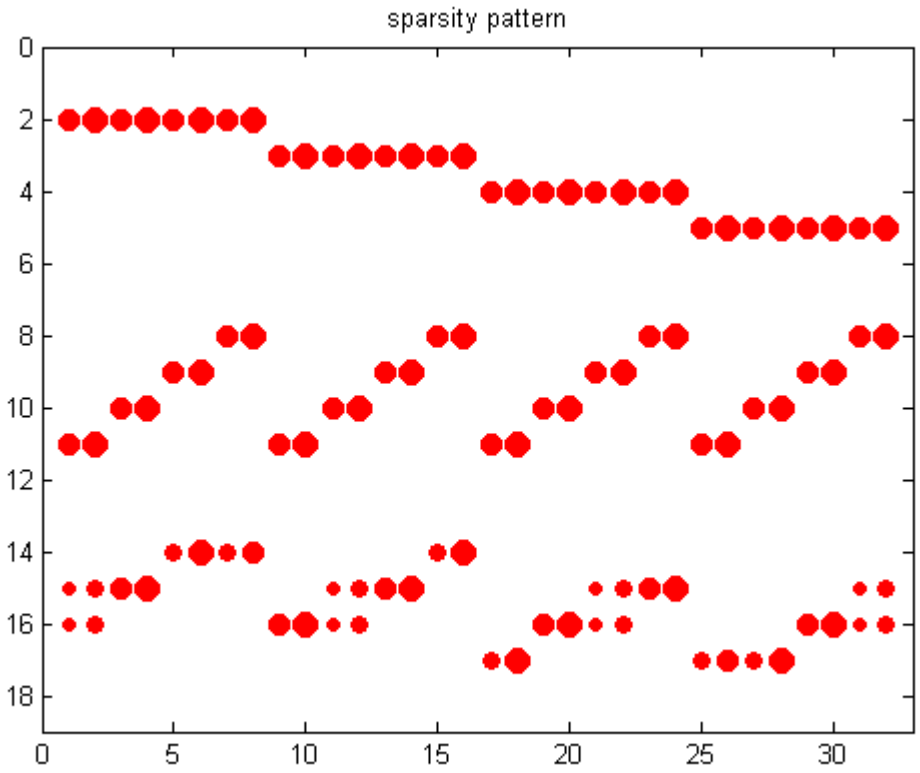

Fig. 2. Sparsity pattern of the matrix of constraints for an image 4x4 (N=4) and 3 projections, number of detector pixels $\sqrt{2}$N and detector width $\sqrt{2}$N.

2.1.1. Extension to multiple solid phases.

The proposed methodology has been presented for the case of two mineralogical species aforementioned with the labels L and H. However, in the real word of mineral processing the operator rarely deals with one single valuable phase (H) and most frequently with solid particles containing several mineral species (i.e. multi-phase particles). Some phases may be valuable others may be penalizing impurities for the concentrate-smelter. In X-ray computed tomography a prerequisite for 'sensing' the different phases is the diverse attenuation to the X-rays; that is usually attained when there exists a good contrast in their density. Two different mineral species with very close density cannot be distinguished by X-ray tomography.

In the case in which a particle bears two species of interest with different density -e.g. linear attenuation H1 and H2 in addition to the gangue L, the model presented above can be straight-forward extended provided that the equality (3) -introducing the new Boolean variable y - is re-written as :

$$\dots s_{i,j}\, L\, y_k + s_{i,j}\, H1\, y_{k+1} + s_{i,j}\, H2\, y_{k+2} \dots = p_i \tag{7}$$

with:

$$y_k + y_{k+1} + y_{k+2} \leq 1 \tag{8}$$

These constraints prescribe that a pixel can be H1 or H2 or L or 0.

The DART problem is solved as a Boolean problem, with y taking values in {0 , 1}. The binary solution y is then post-processed as:

$$\begin{cases} \text{if } y_k = 0 \; and \; y_{k+1} = 0 \; and \; y_{k+2} = 0 \; then \; x_j = 0 \\ \text{if } y_k = 1 \; and \; y_{k+1} = 0 \; and \; y_{k+2} = 0 \; then \; x_j = L \\ \text{if } y_k = 0 \; and \; y_{k+1} = 1 \; and \; y_{k+2} = 0 \; then \; x_j = H1 \\ \text{if } y_k = 0 \; and \; y_{k+1} = 0 \; and \; y_{k+2} = 1 \; then \; x_j = H2 \end{cases} \quad (9)$$

This extension does add computational complexity to the problem but the solution remains at reach of a workstation.

The proposed DART method can be extended to distinguish even more mineral species by intuitive modifications of Equations (7-9).

3.Numerical examples

In this section the DART method proposed for fast tomographic reconstruction is demonstrated with a more complex numerical example. The aim is to reconstruct a slice of a sample of composite particles containing particles of pure phase L, pure phase H and middling particles both looked and exposing the inclusions. The phantom image is 512 x 512 (N=512). In Fig. 3 the phantom and the corresponding DART reconstruction with 36 projections, are reported. The sparsity of the tomographic system matrix (denoted with S in Eq.(1)) is 0.003. The reconstructed image allows to recognize the mineralogical phase inclusions.

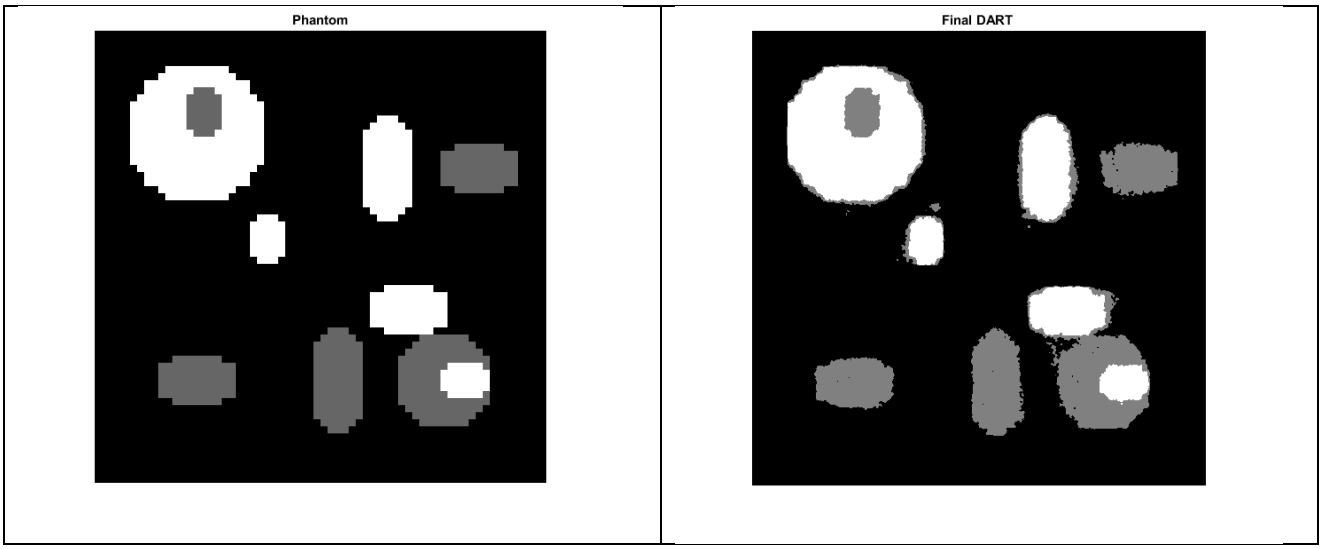

Figure 3. Left: Composite particles 512X512 pixels phantom. Right: DART reconstruction with 36 projections.

For comparison in Fig. 4 the classical FBP reconstructions obtained with 36 projections (the same number of projections used for DART) and 1170 projections ($3.14/2\sqrt{2}\,512$ as prescribed by Nyquist to avoid under-sampling when using FBP) are reported. The FBP reconstruction is obtained with a detector width $\sqrt{2}$N and number of detector pixel $\sqrt{2}$N. The FBP reconstructed with 36 projection (Fig. 4, left side) allows qualitative recognition of the type of particle but cannot be segmented automatically; it still contains artifacts that can be extinguished only with hundreds of projection.

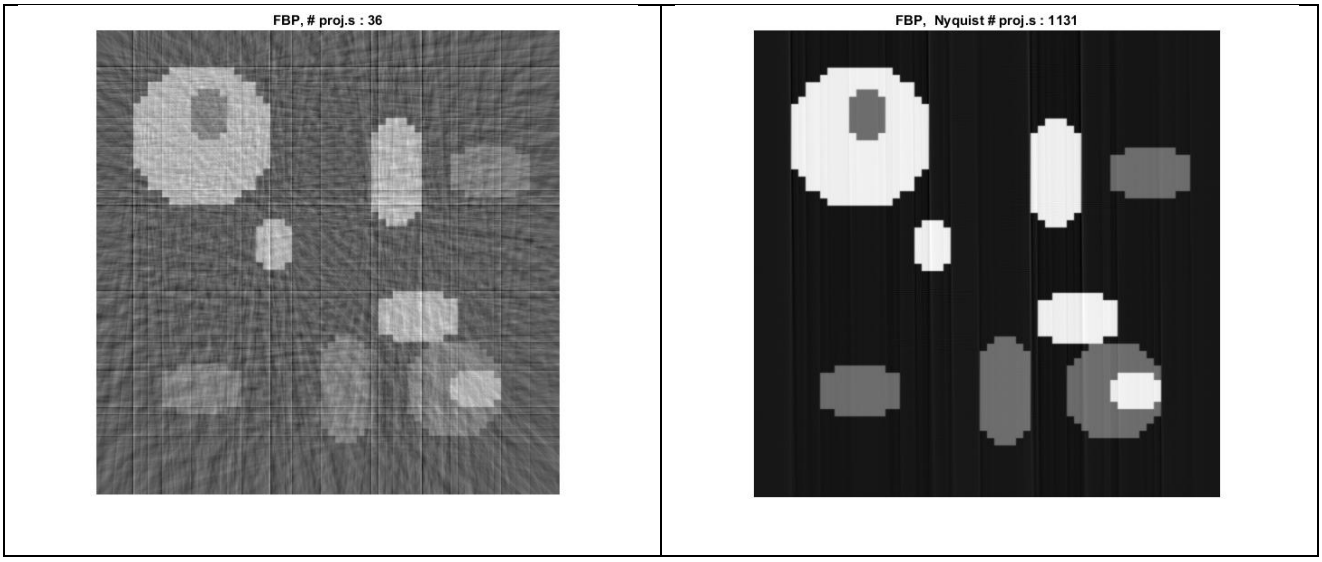

Fig. 4. Left: Filter Back Projection reconstruction with 36 projections. Right: FBP reconstruction with 1170 projections.

In Fig. 5 the error image shows the pixels different in the DART reconstructed image from the correspondent pixels on the phantom . Darker pixels represent values in the reconstructed that exceed the pixel value in the phantom. Vice-versa brighter pixels are those with a lower value. The relative mean error (RME) is 2.4 percent , it is the number of pixels different in the reconstruction and in the original phantom to all the pixels in the original phantom.

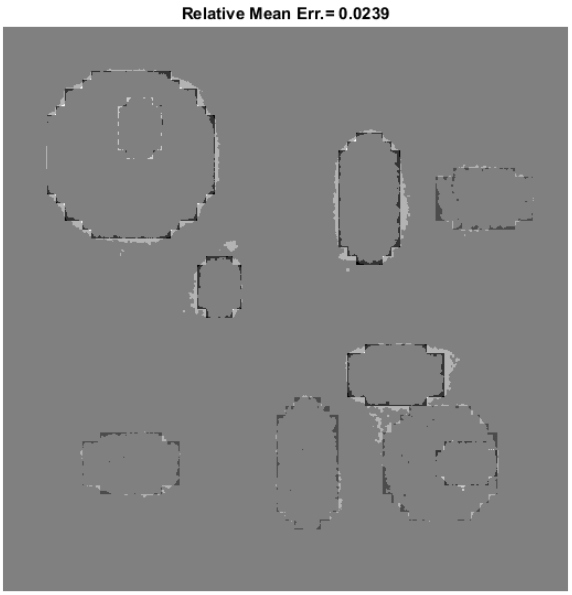

Fig. 5. Reconstruction error image. The RME is 2.4 percent.

The relative error decreases further at the increase of the number of projection view angles but the computational effort for the solution of the problem increases as a consequence and requires major hardware resources. The reconstructions reported in this paper were obtained with a low-cost workstation based on a multi core E5 Intel Xeon processor. We consider that the size (512 x 512) and the number of projections (40 circa) is the maximum amenable by our hardware. A synthetic pseudocode of the software is reported in Appendix A.

4.Conclusions

Preliminary numerical experiments on synthetic data show that DART methods offer the possibility to limit the number of X-ray projections necessary to reconstruct a slice image in a tomographic system applied to the characterization of composite particles. By and large, our initial experiences show that discrete tomography cast around the algebraical reconstruction methods allows reconstructions with one fraction of the number of projections required by the traditional continuous filtered back projection method that is in use today. In turn, the scanning time -that is the bottleneck of a tomographic acquisition- is reduced proportionally. Conservatively assuming that one X-ray projection requires two seconds of radiographic exposition, the implementation of these findings paves the way for the characterization of a particulate systems in minutes from the collection of the sample thus providing an information of higher values for plant optimization/tuning.

Here the proposed DART method is demonstrated numerically with a two mineralogical phase synthetic sample. In section *2.1.1*. it is shown as it can be extended also to a scanned object consisting of more mineralogical phases each corresponding to a constant grey value in the reconstruction. Prior knowledge of the grey values for each of the mineralogical phase is necessary to pilot image reconstruction towards a slice that contains only these grey values. This prior knowledge can be easily attained with the use of one single traditional (i.e. continuous) tomography.

The discrete tomography method proposed still requires validation with real noisy tomographic projections and comparison with continuous tomography. This is currently under investigation. Undoubtedly the numerical preliminary experiments show that also a limited set of projections encompass the information sufficient to recover the sample morphological and mineralogical composition and that methods of tomographic reconstruction alternative to those in use today deserve attention.

No modification of the hardware of the existing X-CT machines is required. In addition -due to the lower number of projections taken- the X-ray detector component is subjected to less stress and lasts longer.

References

Barbery,G., 1991
Mineral liberation: measurement, simulation and practical use in mineral processing.
Éditions GB, Quebec, Canada, 351 pages

Batenburg, K.J., Sijbers, J., 2011
DART: A Practical Reconstruction Algorithm for Discrete Tomography.
IEEE Transactions on image processing, vol. 20, No. 9, 2542-2543

Baum, W., 2014
Ore characterization, process mineralogy and lab automation a roadmap for future mining.
Minerals Engineering, vol. 60, 69–73

Casagrande, D., Piller, M., Santini, M., Schena, G. , 2014
Characterisation of water-oil drainage process through a reservoir rock sample by digital core analysis.
International Journal of Oil, Gas and Coal Technology , vol. 8 , Issue 4, 399 - 416

Chiaruttini,C., Piga,L., Schena,G. , 1999
An assessment of the efficiency of a stereological correction for recovering the volumetric grade of particles from measures on polished sections.
International Journal of Mineral Processing, vol. 57, Issue 4, 303-322

Dhawan, N.,Safarzadeh, M.S., Miller,J.D. , Moats, M.S., Rajamani, R.K., Lin, C.L. , 2012
Recent advances in the application of X-ray computed tomography in the analysis of heap leaching systems.
Mineral Engineering, vol. 35, 75-86

Gabor T Herman, Attila Kuba, (Eds.), 2007
Advances in Discrete Tomography and Its Applications.
Series: Applied and Numerical Harmonic Analysis , 392 pages
Birkhäuser Basel

Lin, C.L.,Miller, J.D. , 1996
Cone beam X-ray microtomography for three-dimensional liberation analysis in the 21st century.
International Journal of Mineral Processing, vol. 47, Issue 1-2, 61-73

Lin, C.L.,Miller, J.D. , 2000
Network analysis of filter cake pore structure by high resolution X-ray micro-tomography.
Chemical Engineering Journal, vol. 77, Issue 1-2, 79-86

Leigh, G.M., Lyman, G.J. , Gottlieb, P. , 1996
Stereological estimates of liberation from mineral section measurements: a re-derivation of Barbery's formulae with extensions.
Powder Technology, vol. 87, no. 2, pp. 141–152

Miller, J. D. , Lin, C. L., 2003
3D analysis of particulates in mineral processing systems by cone beam X-ray microtomography.

in Lorenzen, L., Bradshaw, D. J., Aldrich, C., Eksteen, J. J., Wright, M., & Thom, E. (Eds.), Proceedings of XXII International Mineral Processing Congress: 29 September - 3 October 2003, Cape Town, South Africa. 1561-1570.

Miller, J.D. ,Lin, C.L., Hupka, L., Al-Wakeel, M.I., 2009
Liberation-limited grade/recovery curves from X-ray micro CT analysis of feed material for the evaluation of separation efficiency.
International Journal of Mineral Processing, vol. 93, Issue 1, 48-53

Pan, X., Sidky, EY., Vannier, M., 2009
Why do commercial CT scanners still employ traditional filtered back-projection for image reconstruction?
Inverse Problems , 25(12), doi:10.1088/0266-5611/25/12/123009

Piller, M., Schena, G., Nolich, M., Radaelli, F., Rossi, E., 2009
Analysis of hydraulic permeability in porous media: from high resolution X-ray tomography to direct numerical simulation.
Transport in porous media, vol. 80, Issue 1, pp.57-78. 0169-3913

Schena,G. and Montanari,F. , 2003
Toward a mineral liberation sensor.
in Lorenzen, L., Bradshaw, D. J., Aldrich, C., Eksteen, J. J., Wright, M., & Thom, E. eds. Proceedings of XXII International Mineral Processing Congress: 29 September - 3 October 2003, Cape Town, South Africa, Vol 1, 162-170, ISBN-10(13): 0 958 46092 2

Schena,G., Santoro,L., Favretto,S., 2007
Conceiving a high resolution and fast X-ray CT system for imaging fine multi-phase mineral particles and retrieving mineral liberation spectra.
International Journal of Mineral Processing, vol. 84, Issues 1–4, 327-336

Schena,G., Favretto,S., Santoro,L., Pasini,A., Bettuzzi,M., Casali,F., Mancini,L., 2005
Detecting microdiamonds in kimberlite drill-hole cores by computed tomography.
International Journal of Mineral Processing, vol. 75, Issues 3–4, 173–188

Van Aarle, W., Batenburg, K.J., Sijbers J., 2012
Automatic Parameter Estimation for the Discrete Algebraic Reconstruction Technique (DART).
IEEE Transactions on image processing, vol. 21, No. 11

APPENDIX A

```
% Img is the NxN slice image sought
% Sys is the tomographic system matrix NxN columns as defined in Eq. 1
% L & H are the X-ray linerar attenuation coef. of the low and high density mineral species
% N_proj is the number of projection rays
N_pix=N*N; % number of unknown pixel values
N_fs=20; % Number feasible solutions

parfor i: 1: N_fs % parallel loop to generate and save feasible solutions
  r=randperm(N_proj); %generate one randon permutation of integers 1:N_proj
  %build new matrix with projection order given by r by re-arranging the rows of Sys
  Aeq(r,1:2:N_pix*2-1) =Sys(:,1:N_pix).*L; % Eq. 3
  Aeq(r,2:2:N_pix*2)   =Sys(:,1:N_pix).*H; % Eq. 3
  Aeq =[Aeq; B]; % append matrix B constraining pixel values to be 0 or L or H, Eq. 4
  beq=[Proj;ones(N_pix,1)]; % append ones to projection vector data, Eq. 4 right side
  Y=solve_blp(Aeq,Proj); %solve binaly linerar problem
  X=convert(Y); % convert binary solution to discrete values Eq. 5
  save(filename(i));% save binary solutions X
end % end parallel for loop

% load files to retrive N_fs solutions X and sum up X_sum
X=X_sum/N_fs; % normalize to L and H
% Img=reshape(X,[N,N]); % convert DART solution to square NxN image
% Img is the DART solution image
```

Appendix 1 is a Matlab style informal pseudo-code with a synthetic high-level description of the operating principle of the DART algorithm proposed.

Figure

Click here to download high resolution image

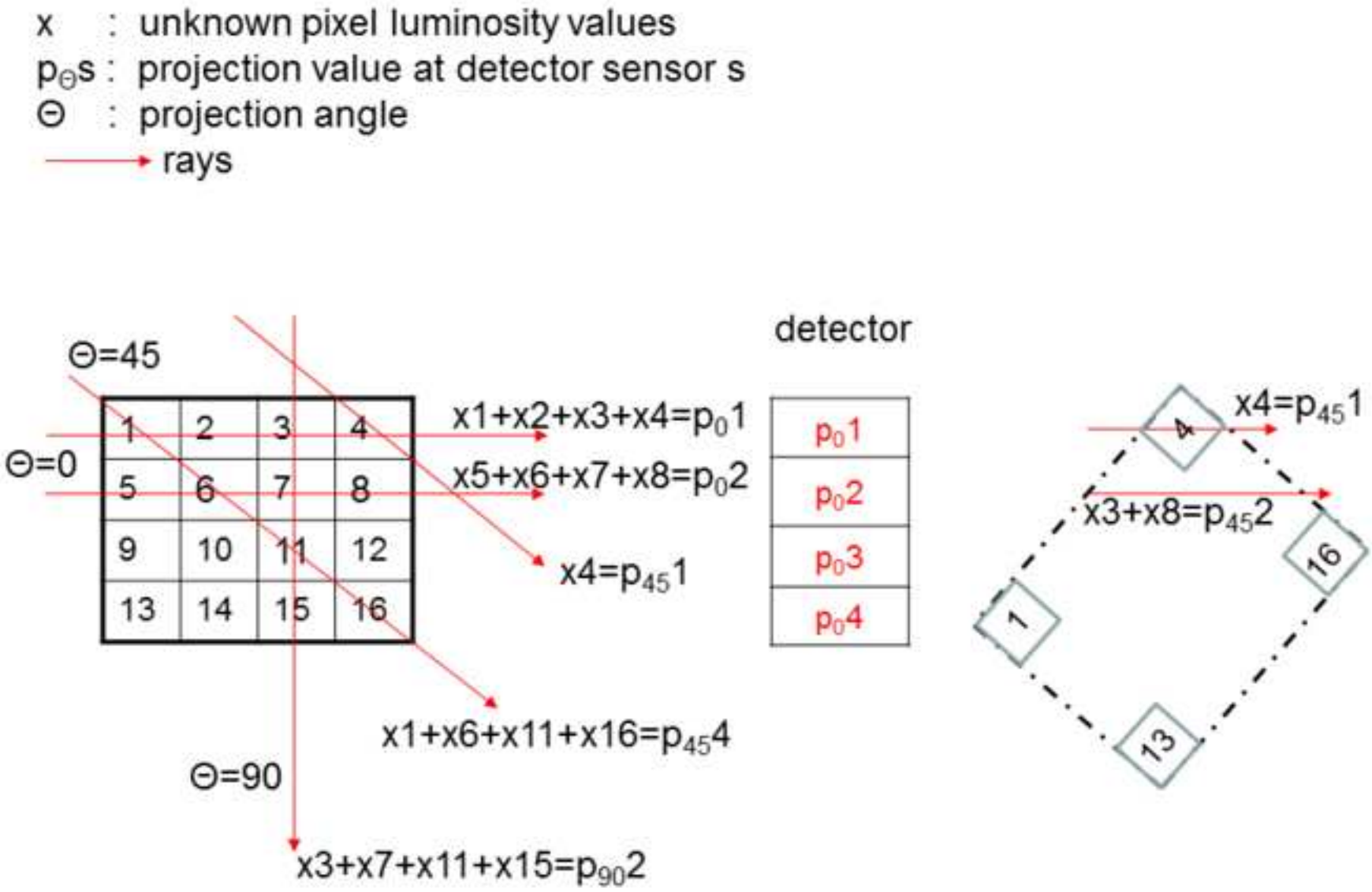

Figure

Click here to download high resolution image

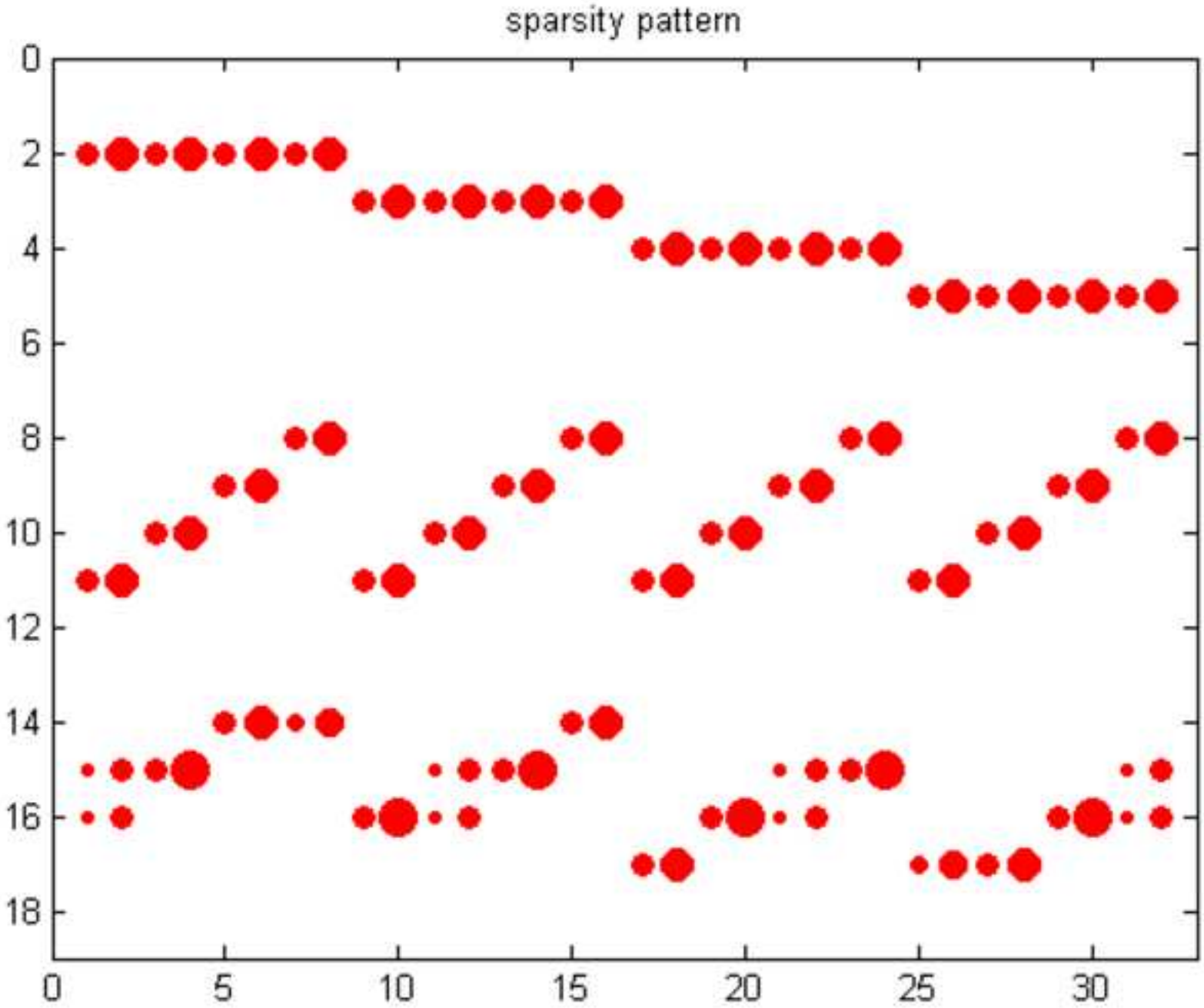

Figure

Click here to download high resolution image

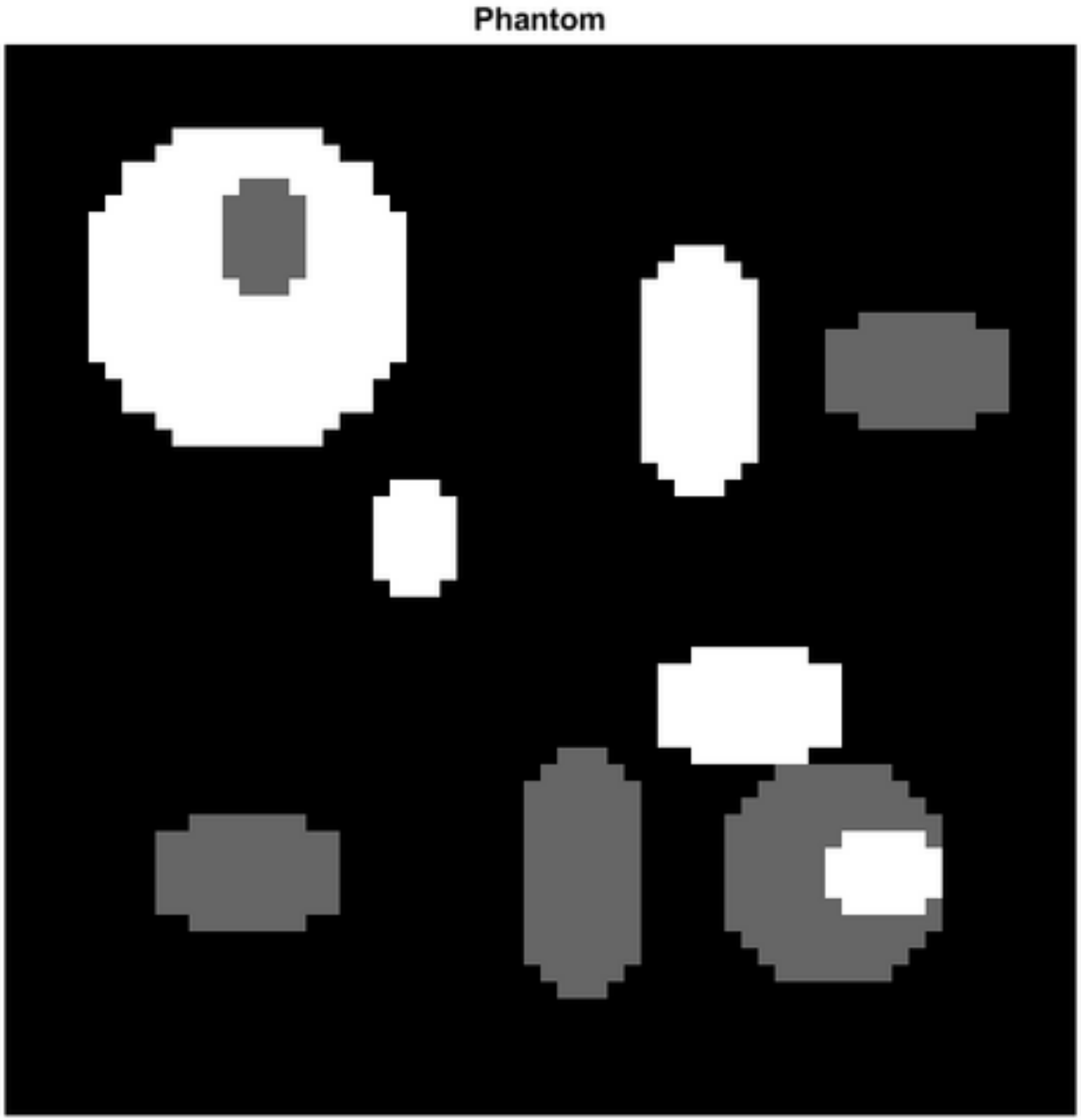

Figure

Click here to download high resolution image

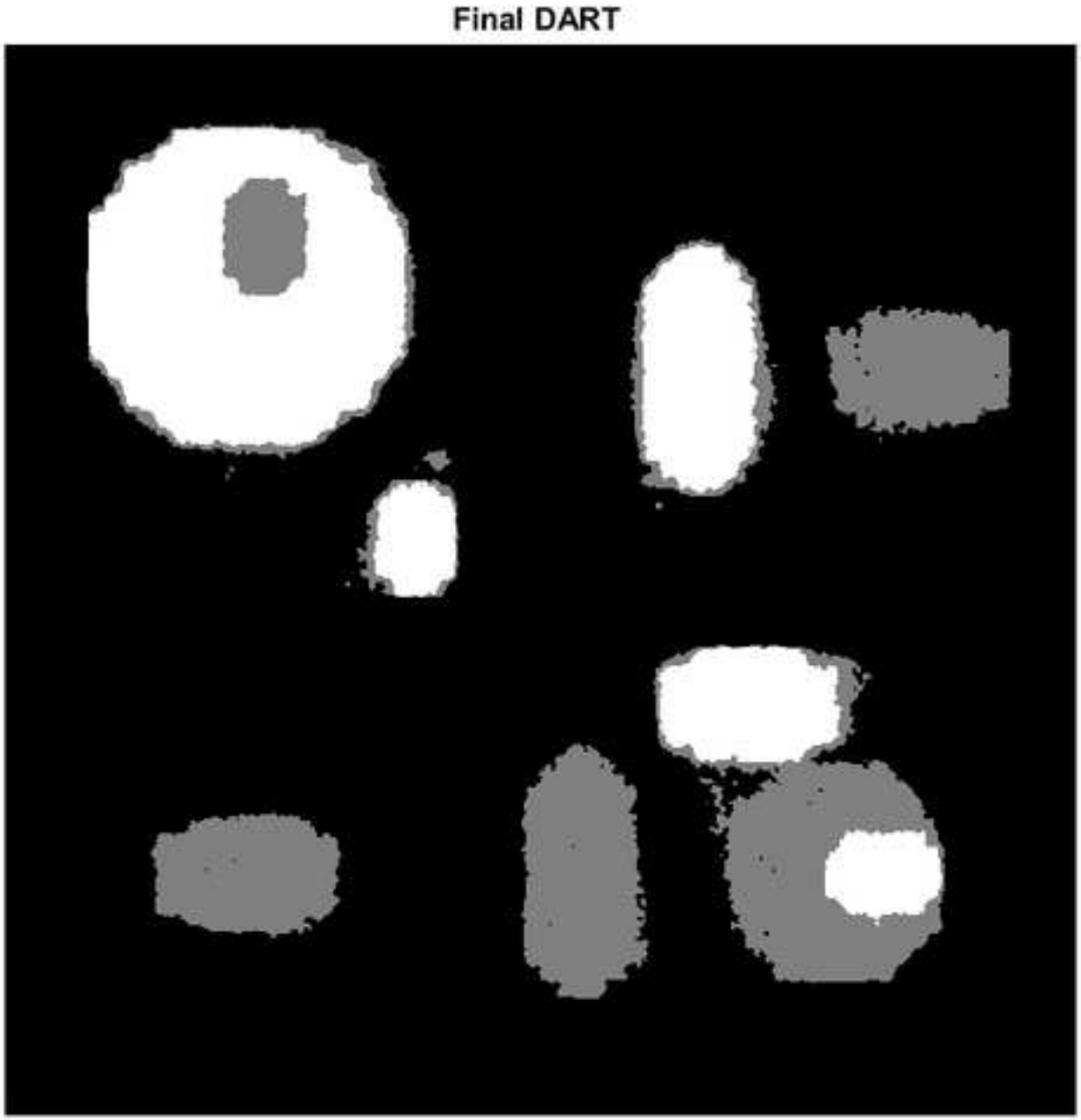

Figure

Click here to download high resolution image

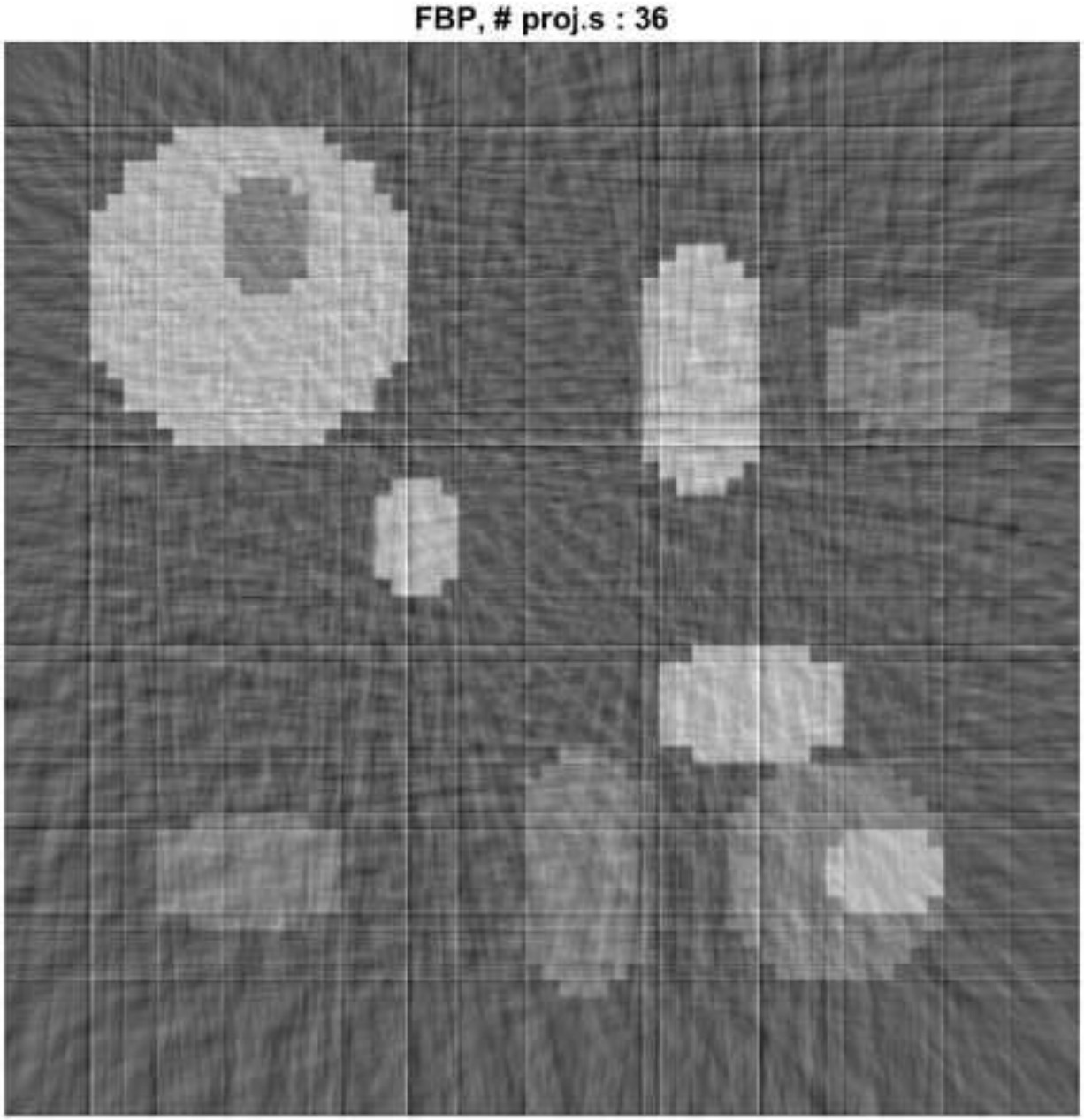

Figure

Click here to download high resolution image

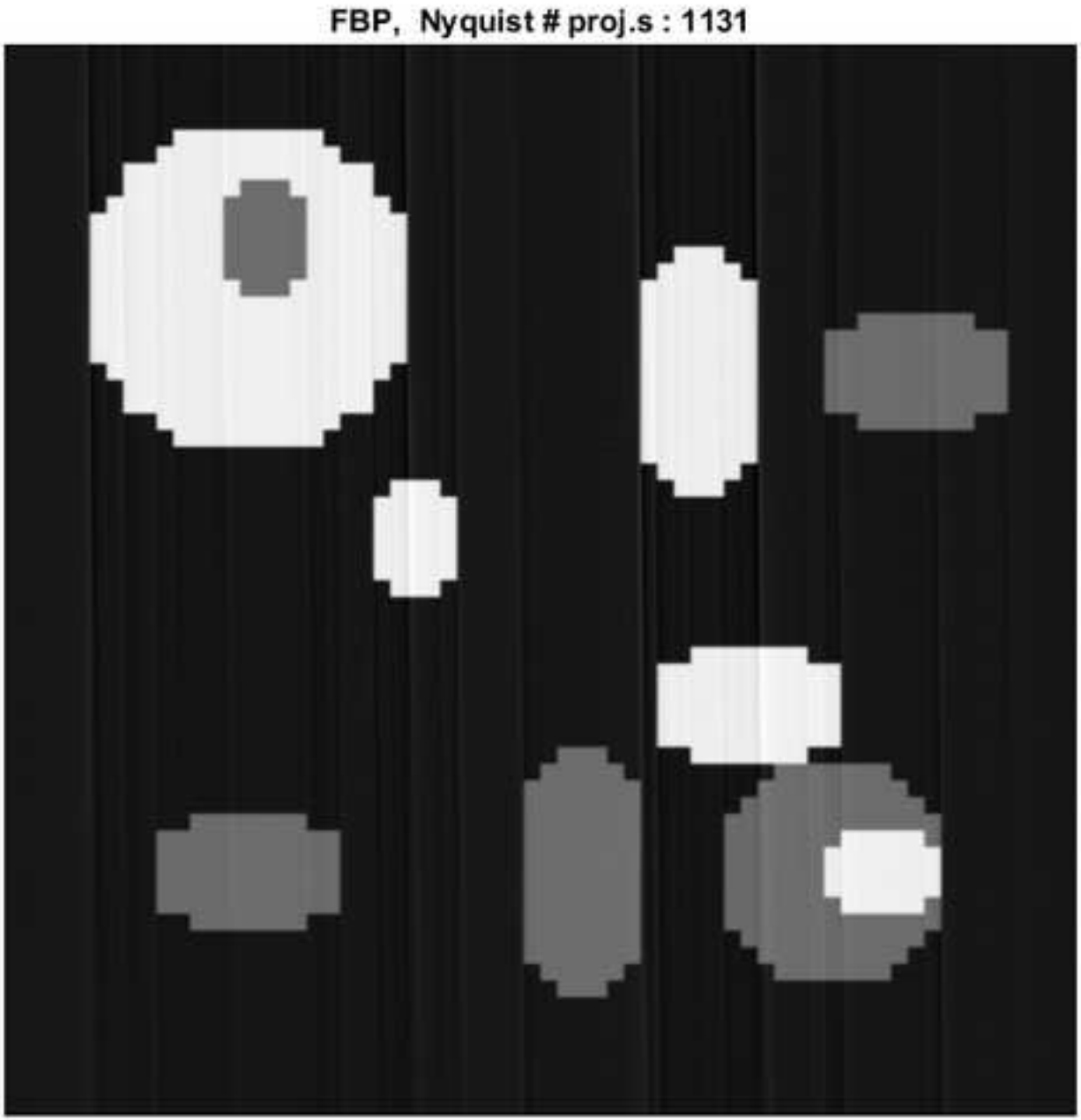

Figure

Click here to download high resolution image